*Proc. Natl. Acad. Sci. USA*
Vol. 96, pp. 4432–4437, April 1999
Cell Biology

# Tamoxifen inhibits acidification in cells independent of the estrogen receptor

**(pH/multidrug resistance/breast cancer/bone resorption)**

NIHAL ALTAN*†‡, YU CHEN*‡, MELVIN SCHINDLER§, AND SANFORD M. SIMON*¶

*Laboratory of Cellular Biophysics, The Rockefeller University, 1230 York Avenue, New York, NY 10021; and §Department of Biochemistry, Michigan State University, East Lansing, MI 48824

*Communicated by Günter Blobel, The Rockefeller University, New York, NY, February 17, 1999 (received for review January 22, 1999)*

**ABSTRACT** **Tamoxifen has been reported to have numerous physiological effects that are independent of the estrogen receptor, including sensitization of resistant tumor cells to many chemotherapeutic agents. Drug-resistant cells sequester weak base chemotherapeutics in acidic organelles away from their sites of action in the cytosol and nucleus. This work reports that tamoxifen causes redistribution of weak base chemotherapeutics from acidic organelles to the nucleus in drug-resistant cells. Agents that disrupt organelle acidification (e.g., monensin, bafilomycin $A_1$) cause a similar redistribution. Measurement of cellular pH in several cell lines reveals that tamoxifen inhibits acidification of endosomes and lysosomes without affecting cytoplasmic pH. Similar to monensin, tamoxifen decreased the rate of vesicular transport though the recycling and secretory pathways. Organellar acidification is required for many cellular functions, and its disruption could account for many of the side effects of tamoxifen.**

Breast cancer afflicts 1 in 8 women and in the Western world it is the most common form of cancer in women (1). Most breast cancers depend on estrogen for growth. Tamoxifen, commonly known for its activity as a nonsteroidal modulator of the estrogen receptor, is the most widely prescribed treatment for breast cancer in the United States (2).

Tamoxifen currently is used both for treatment against metastatic breast tumor and for long-term adjuvant therapy after the primary tumor has been removed by surgery (3). In addition, tamoxifen therapy decreases the incidence of primary tumors in the contralateral breast. This and other findings have motivated the widespread use of tamoxifen as a long-term chemopreventative agent against breast cancer (4). Initial results showed that long-term tamoxifen treatment significantly decreased the incidence of breast cancer. However, it also demonstrated a number of serious side effects (5).

Although tamoxifen was discovered as an estrogen receptor antagonist, years of clinical experience and basic science research have unveiled a number of other effects (6). Some effects are proestrogenic and are thought to be caused by the ability of tamoxifen to act as a partial agonist in some tissues. Beneficially, tamoxifen slows the development of osteoporosis and atherosclerotic heart disease and alleviates many symptoms of menopause (7). But detrimentally, it significantly increases the risks for thrombotic events (e.g., pulmonary embolism, embolic stroke, and thrombophlebitis), endometrial cancer (2), liver disease, and liver cancer (8).

Importantly, tamoxifen has been shown to possess activities that are independent of the estrogen receptor: decreasing the level of cyclic nucleotides (9), binding and inhibiting protein kinase C (10), binding to calmodulin and inhibiting cAMP phosphodiesterase activation, and partitioning into lipids where it exerts antioxidant and membrane fluidizing activities (11). Yet, there are clinically significant actions of tamoxifen for which the biochemical mechanism still remains obscure. These include: (*i*) resensitization to chemotherapeutics of both estrogen receptor positive and negative multidrug resistant tumor cells *in vitro* and *in vivo* (12, 13), (*ii*) modulation of several families of secreted protease activities implicated in tumor invasion and metastasis, including cathepsin D, collagenase, and urokinase plasminogen activator (14–16), (*iii*) modulation of cell adhesion to extracellular matrix (17–19), (*iv*) modulation of responsiveness and secretion to a number of growth factors (20–24), (*v*) carcinogenic effects both *in vitro* and *in vivo* on the liver and uterus both in animal studies and humans (2, 8), (*vi*) inhibition of a number of membrane channels and transporters (25–31), and (*vii*) inhibition of bone resorption (32, 33). The diverse array of effects attributed to tamoxifen suggests the possible existence of a more fundamental mechanism with many downstream consequences.

The results reported in this paper originate from studies on chemotherapy resistance in tumor cells. The chemotherapeutic Adriamycin localizes in acidic intracellular organelles in drug-resistant cells but is dispersed throughout the cytoplasm and nucleus in drug-sensitive cells (34–38). Drug-sensitive cells have fewer acidic organelles than resistant cells. Disruption of the pH of acidic organelles in resistant cells with the protonophore monensin, the proton pump inhibitor bafilomycin $A_1$, or the lysosomotropic agent chloroquine both reverses the phenotype of drug distribution and reverses drug resistance (36–38). The observation that tamoxifen reverses multidrug resistance led us to examine its effect on organelle acidification.

In this paper we report that, like monensin and bafilomycin $A_1$, tamoxifen increases sensitivity of drug-resistant breast cancer cells to Adriamycin and causes a redistribution of cellular Adriamycin from acidic organelles to the nucleus. Quantitative measurement of subcellular pH shows that tamoxifen causes alkalinization of acidic organelles without significantly affecting cytosolic or nuclear pH. Inhibition of organelle acidification by tamoxifen occurs in all cells examined and depends on neither the estrogen receptor nor P-glycoprotein. Furthermore, cells treated with tamoxifen showed the physiological sequelae of defective acidification—slowed transport through both the endocytic and biosynthetic pathway.

Abbreviations: TGN, trans-Golgi network; AO, acridine orange; SNARF, seminaphthorhodafluor; DAMP, *N*-(3-[(2,4-dinitrophenyl)amino]propyl)-*N*-(3-aminopropyl)methylamine dihydrochloride; DNP, dinitrophenol.

†Present address: Cell Biology and Metabolism Branch, National Institute of Child Health and Human Development, National Institutes of Health, Bethesda, MD 20892.
‡N.A. and Y.C. contributed equally to this work.
¶To whom reprint requests should be addressed. e-mail: simon@rockvax.rockefeller.edu.

The publication costs of this article were defrayed in part by page charge payment. This article must therefore be hereby marked "*advertisement*" in accordance with 18 U.S.C. §1734 solely to indicate this fact.

PNAS is available online at www.pnas.org.

## MATERIALS AND METHODS

**Materials.** Bafilomycin $A_1$, monensin, acridine orange (AO), tamoxifen, and nigericin were from Sigma. BODIPY-transferrin, BODIPY-ceramide, FITC-transferrin, seminaphthorhodafluor (SNARF)-dextran, *N*-(3-[(2,4-dinitrophenyl)-amino]propyl)-*N*-(3-aminopropyl)methylamine dihydrochloride (DAMP), Hoechst 33258, LysoSensor Blue DND167, and FITC-dextran were from Molecular Probes. Adriamycin was from Calbiochem. Concanomycin A was from Fluka. Mouse anti-dinitrophenol (DNP) antibody was from Oxford Biomedical Research (Oxford, MI). Gold-conjugated anti-mouse secondary antibody was from Amersham Pharmacia.

**Cell Culture.** Cells were seeded and grown in DMEM containing 10% FCS (phenol red free) in Lab-Tek coverslip culture chambers (Nalge) or on coverslips and maintained in an incubator at 37°C and 5% $CO_2$. Human breast cancer cells (MCF-7, MDA-231) and the Adriamycin-resistant lines (MCF-7/ADR, MDA-A1) were obtained from William W. Wells of Michigan State University (East Lansing) and the American Type Culture Collection. Be(2) and Be(2)ADR neuroblastoma cells were obtained from June L. Biedler (Fordham University, New York). The medium for the MCF-7/ADR cells was supplemented with Adriamycin (0.5 $\mu$g/ml). Cells were used 3–4 days after plating.

**Microscopy.** Unless otherwise indicated, all microscopy and treatments were done with medium at 37°C and equilibrated with 5% $CO_2$. The cells remained stable for many hours, allowing the effects of a variety of media and reagents to be assayed on the same field of cells. For confocal microscopy, 0.5-$\mu$m optical sections were taken with an Ultima Laser Scanning Confocal Microscope (Meridian Instruments, Okemos, MI). In some experiments cells were observed under epifluorescence by using either an Olympus IX-70 inverted microscope and a cooled charge-coupled device (CCD) camera (Hamamatsu Photonics model 4742–95, Hamamatsu City, Japan) or a Nikon Diaphot inverted microscope and an intensified CCD camera (Hamamatsu Photonics model C5909). Images were collected and analyzed with software written in LABVIEW (National Instruments, Austin, TX).

**Labeling of Cells with Adriamycin.** Cells were loaded with Adriamycin (10 $\mu$M) added to the perfusion medium. Adriamycin fluorescence was imaged with the confocal microscope with $\lambda_{ex}$ = 488 nm.

**Labeling of Cells with AO.** Cells were incubated with AO (6 $\mu$M in medium from a 10 mM stock in water) for 15 min and then examined with $\lambda_{ex}$ = 488 nm, and dual emission confocal images were simultaneously recorded with $\lambda_{em}$ = 530/30 nm (green fluorescence) and $\lambda_{em}$ = 605/LP nm (red fluorescence).

**Organelle-Specific pH Measurements.** The pH was measured in selective cellular compartments by targeting ratiometric pH probes to specific organelles as described (38). On the confocal microscope, the pH probe SNARF was studied with $\lambda_{ex}$ = 514 nm, and emission was recorded simultaneously by using a 610-nm dichroic with both a 570/30-nm and a 630/LP-nm filter. By using a Nikon epifluorescence microscope with an intensified charge-coupled device camera, the pH probe FITC was excited alternately at 450 nm and 490 nm with $\lambda_{em}$ = 520/10 nm. In each experiment the emission of the dyes were calibrated as a function of pH as described (38). To calibrate the pH for the endosomal system, the chamber was perfused with 150 mM sodium buffers at pH of 5, 6, or 7 containing monensin (20 $\mu$M) and nigericin (10 $\mu$M) for 5 min before recording the fluorescence. For the pH calibrations of cytosol and nucleoplasm, the cells were incubated in 140 mM potassium buffers at pH 6.0, 6.5, 7.0, and 7.5 containing nigericin (20 $\mu$M).

*pH in the recycling endosomes.* Cells growing in Lab-Tek chambers were incubated with FITC-transferrin (150 $\mu$g/ml in DMEM/20 mM Hepes, pH 7.3) for 25 min, washed in quick succession 3× with DMEM/Hepes and 3× with Hanks' balanced salt solution/Hepes, and imaged (39).

*pH in the lysosomes.* The pH in the lysosomes was assayed both with light and electron microscopy. For light microscopy, cells were incubated with 10-kDA FITC-dextran (5 mg/ml) (DMEM/Hepes) for 30 min, washed 4× with DMEM/Hepes, and incubated for an additional 90 min to chase the FITC-dextran out of the endosomes and into the lysosomes. They were visualized on a Nikon Diaphot equipped with FITC excitation filters (40). The pH was calibrated as described above. LysoSensor Blue labeling was done exactly as described (38). For electron microscopy, the cells were incubated (±10 $\mu$M tamoxifen) with the weak base DAMP (70 $\mu$M), fixed, probed with a mouse antibody to DNP (crossreacts with DAMP), reacted with gold-conjugated anti-mouse antibodies, and visualized in electron microscopy as described (41).

*pH in the cytosol or nucleus.* The ratiometric pH probe SNARF conjugated to dextran was scrape-loaded into the cytosolic compartment as described (38, 42). The 70-kDa SNARF-dextran selectively reported the cytosolic pH, and the 10-kDa dextran reported both nuclear and cytosolic compartments. Confocal optical sections were used to select nuclear emission.

**Transport Assays.** *Transport of transferrin from recycling endosomes to cell surface.* Transferrin was used to selectively label the recycling endosomes of cells (38, 43). The fluorophore BODIPY was used as a probe because it is fluorescence insensitive to pH changes in the endocytic pathway. Transport of transferrin was assayed as described (43). Cells growing in Lab-Tek chambers were loaded with 25 $\mu$g/ml of BODIPY-transferrin (DMEM/Hepes, pH 7.3, 37°C). After 20 min, the medium was replaced with citric acid buffer (25.5 mM citric acid monohydrate/24.5 mM sodium citrate/280 mM sucrose, pH 4.6) containing 10 $\mu$M deferoxamine mesylate and incubated for 2 min at 37°C to remove plasma membrane-bound BODIPY-transferrin. The cells were rapidly washed 4× with McCoy's 5A medium (20 mM Hepes/50 $\mu$M deferoxamine mesylate/100 $\mu$g/ml of unlabeled human transferrin) and examined on a confocal microscope ($\lambda_{ex}$ = 488, $\lambda_{em}$ = 530) at various time points.

*Transport of sphingomyelin from trans-Golgi network (TGN) to cell surface.* BODIPY-ceramide labels endomembranes and its metabolic product, BODIPY-sphingomyelin, accumulates within the Golgi compartments (44). When accumulated at high concentrations, BODIPY-sphingomyelin undergoes a green to red shift in fluorescence emission. Excitation was at 488 nm, and dual emission images were prepared by using the filter set described for AO and a 100× oil immersion objective. Cells cultured for 3–4 days in Lab-Tek chambers were washed 3× with DMEM (pH 7.2), incubated with BODIPY-ceramide (3 $\mu$g/ml) for 60 min at 37°C/5% $CO_2$, washed 2× with cold DMEM, and then incubated in the absence or presence of tamoxifen (10 $\mu$M) for 15 min on ice. The cells then were incubated for 0, 60, or 120 min at 37°C/5% $CO_2$ in DMEM or DMEM/tamoxifen (10 $\mu$M), fixed (1% paraformaldehyde, 0.1 M sodium cacodylate, 0.1 M sucrose, pH 7.2), and imaged.

## RESULTS

**Effects of Tamoxifen on Adriamycin Localization.** The cellular distribution of chemotherapeutics was assayed by monitoring the localization of the drug Adriamycin. Adriamycin was chosen because it frequently is used in the treatment of breast cancer, is representative of multidrug resistant-sensitive chemotherapeutics, and is naturally fluorescent. In the drug-sensitive MCF-7 cells, Adriamycin is found diffusely throughout the nucleoplasm and cytoplasm (Fig. 1*A*). In contrast, in MCF-7/ADR cells, Adriamycin is observed to be primarily localized within punctate cytoplasmic organelles

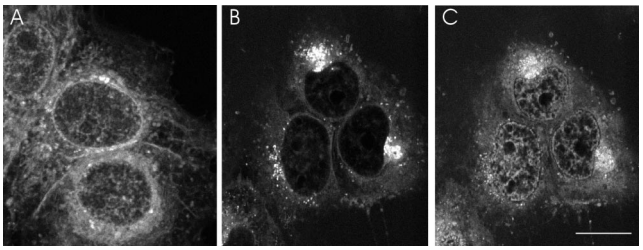


FIG. 1. Steady-state distribution of Adriamycin (*A*) in drug-sensitive MCF-7 cells was diffuse throughout the cytoplasm with an increased fluorescence in the nucleoplasm. (*B*) In drug-resistant MCF-7/ADR cells Adriamycin is excluded from the nucleus and is accumulated in punctate cytoplasmic organelles. (*C*) The MCF-7/ADR cells in *B* were treated with 10 $\mu$M tamoxifen for 30 min, resulting in a redistribution of Adriamycin from the cytoplasmic organelles to the nucleus.

(Fig. 1*B*), which colocalize with the acidified organelles of the cell: lysosomes, TGN, and endosomes (38). Similar differences in distribution of Adriamycin and other chemotherapeutics (e.g., daunorubicin, mitoxantrone) are seen in other pairs of drug-sensitive and drug-resistive tumor cell lines (data not shown). After a 30-min treatment with tamoxifen (10 $\mu$M) the distribution of Adriamycin in MCF-7/ADR cells shifted from punctate cytoplasmic compartments (Fig. 1*B*) to the nucleoplasm and cytoplasm (Fig. 1*C*). This distribution of Adriamycin is similar to that observed in MCF-7 drug-sensitive cells in the absence of tamoxifen (Fig. 1*A*) (36, 38). The effect of tamoxifen on the distribution of Adriamycin was dose dependent and was detectable at 0.5 $\mu$M (data not shown). In the drug-resistant MDA-A1 cells that lack the estrogen receptor (45), tamoxifen caused a similar redistribution of Adriamycin from the punctate cytoplasmic compartments, suggesting that this redistribution is not estrogen receptor dependent (data not shown).

The tamoxifen-induced increase of Adriamycin in the nucleus could be the consequence of either release from the cytoplasmic organelles or fresh drug influx. To distinguish between these possibilities, tamoxifen was added after removing external Adriamycin. After removal from the media, Adriamycin decreased slowly in all intracellular compartments (Fig. 2*A*). However, in the presence of tamoxifen there was a more rapid decrease of Adriamycin in the organelles and an increase of Adriamycin in the nucleus (Fig. 2*B*). This finding indicates that tamoxifen-induced dispersal of the chemotherapeutic drugs from within the cytoplasmic organelles is sufficient to label the nucleus with Adriamycin.

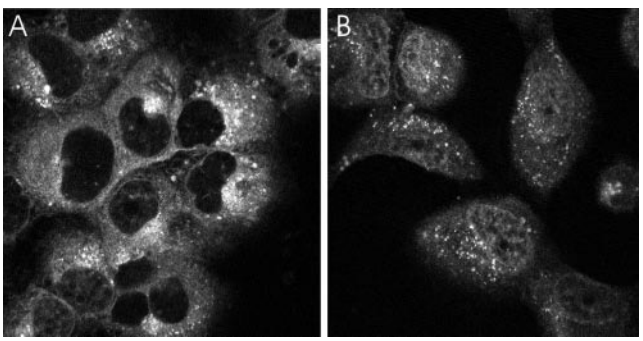


FIG. 2. Washout of Adriamycin from MCF-7/ADR cells. MCF-7/ADR cells were incubated with 10 $\mu$M Adriamycin for 30 min and then rinsed free of external Adriamycin in the absence (*A*) or presence (*B*) of tamoxifen. (*A*) In the absence of tamoxifen, Adriamycin fluorescence slowly decreased after washout. (*B*) The presence of tamoxifen caused decrease in punctate fluorescence in increase in nuclear fluorescence, indicating that Adriamycin diffused out of the punctate compartments into the nucleus and cytoplasm.

**Effects of Tamoxifen on Cellular pH.** *AO.* Because tamoxifen disperses Adriamycin from acidic organelles, experiments were performed to test for an effect of tamoxifen on organelle acidification. AO (41) was used to assay for acidic organelles. It is a weakly basic fluorescent probe that emits green at low concentrations and red at high concentration. AO accumulates in acidic compartments where it fluoresces. In MCF-7/ADR cells AO produced a red fluorescence in the perinuclear position (Fig. 3*B*). This finding is similar to what has been seen in nontransformed cells (38, 46). The addition of 10 $\mu$M tamoxifen for 30 min produced a decrease of the red AO fluorescence in MCF-7/ADR cells (Fig. 3*G* shows the same field of cells as in Fig. 3*B*). This effect also was observed with 1 $\mu$M, 2 $\mu$M, and 5 $\mu$M tamoxifen (data not shown). Similar effects were observed with the protonophores monensin and nigericin or inhibitors of the vacuolar ATPase such as bafilomycin $A_1$ or concanomycin A (38). These findings are consistent with a tamoxifen-mediated reduction of organelle acidification. The AO fluorescence in MCF-7/ADR cells treated with tamoxifen was similar to its fluorescence in MCF-7 drug-sensitive cells (Fig. 3*A*) that are abnormal in organelle acidification (36, 38).

The specificity of the effect of tamoxifen on acidification as assayed by AO was tested on other cell lines, including the MDA-A1 (negative for the estrogen receptor, Fig. 3 *C* and *H*), Be(2)ADR [drug-resistant neuroblastoma cell line that expresses P-glycoprotein (Pgp), Fig. 3 *D* and *I*] and CHO-K1 cells (whose endogenous levels of Pgp are below the limits of detection, ref. 47, Fig. 3 *E* and *J*). In all cells, incubation with AO produces red fluorescence within punctate cytoplasmic organelles and in a perinuclear region (Fig. 3 *C–E*). In all of the cell types studied this red fluorescence was substantially decreased after a 30-min incubation with tamoxifen (Fig. 3 *H–J*). Similar results have been observed in freshly dissociated mouse tail fibroblasts cells (data not shown). These data suggest that the effect of tamoxifen on acidification is independent of both the estrogen receptor and Pgp.

*Quantification of pH in specific organelles.* AO is useful as a qualitative assay of organelle acidification. However, it cannot be used to quantify pH nor to selectively assay the pH in specific compartments. It primarily reports acidification within the lysosomes, the most acidic organelle in the cell. In addition, agents that reverse multidrug resistance potentially could affect AO fluorescence distribution by inhibiting active transport of the probe into organelles or by non-pH-dependent processes. Thus, the pH within different organelles was selectively probed and quantified by using the pH-sensitive dyes SNARF and FITC. These dyes can be used to quantify pH and can be conjugated to probes that can be selectively incorporated into specific organelles of the cell.

To selectively examine the pH within the recycling endocytic vesicles, the ratiometric pH probe FITC was conjugated to transferrin (38, 43). The pH within the recycling endosome compartment is 6.1 in MCF-7/ADR cells (Table 1). After addition of 10 $\mu$M tamoxifen, the pH shifts to 6.7. These results indicate that the endocytic pathway is one of the compartments whose pH was affected by tamoxifen treatment. These results confirm that the effects of tamoxifen on AO fluorescence are the consequence of a change of organelle pH rather than a direct effect on AO.

To selectively label the lysosomes, cells were exposed for 1 hr to FITC conjugated to dextrans. Dextrans enter the cell through endocytosis and are sorted to the lysosomes. After a chase of 1 hr there is no remaining fluorescence within the endosomes. The pattern of dextran loading match that of the lysosomal dye LysoSensor Blue DND167 (data not shown). The pH reported by FITC-dextran in the MCF-7/ADR cells was $5.2 \pm 0.1$. After incubation with 10 $\mu$M tamoxifen, the pH shifted to 6.6 (Table 1).

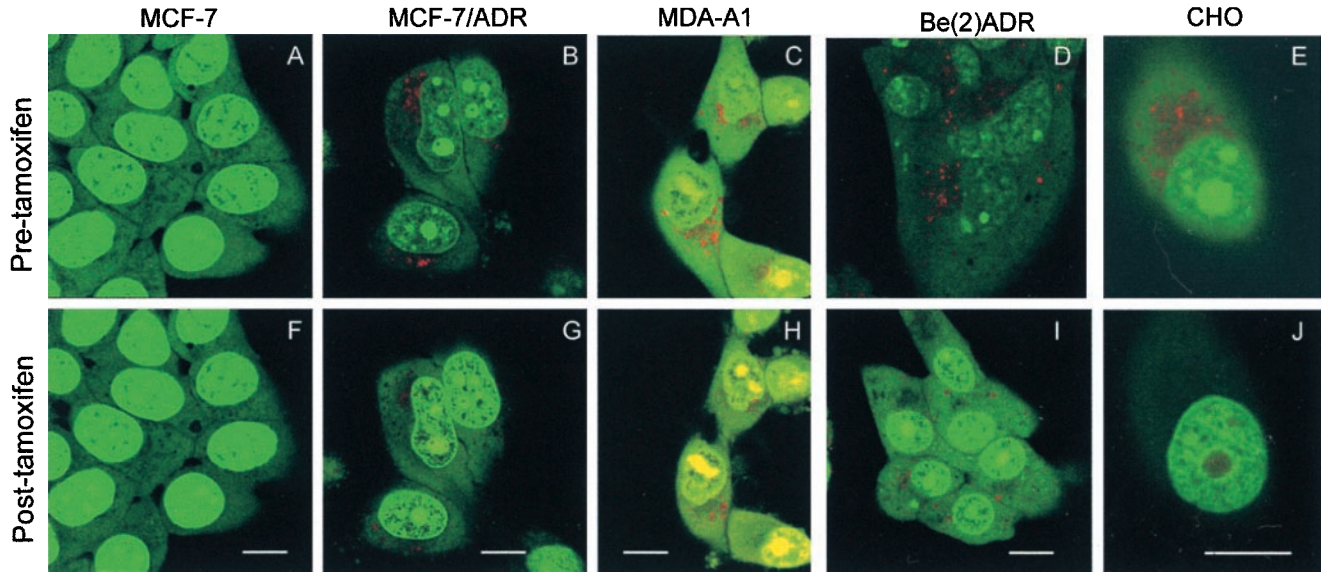


FIG. 3. AO labeling of MCF-7/ADR cells. AO accumulates in acidic compartments, producing a red fluorescence. (*A*) In drug-sensitive MCF-7 cells the AO fluorescence was a relatively even green with no red-orange fluorescence. Punctate red-orange fluorescence, indicative of acidified organelles, was observed in the cytoplasm of: (*B*) drug-resistant MCF-7/ADR breast tumor line, (*C*) drug-resistant (estrogen-receptor negative) MDA-A1 cells breast tumor line, (*D*) drug-resistant Be(2)ADR neuroblastoma cell line, and (*E*) Chinese hamster ovary (CHO) cell line. (*F*) Tamoxifen had no effect on the fluorescence of MCF-7 cells. However, 30 min after the addition of 5 $\mu$M tamoxifen there was a reduction in the red-orange fluorescence in the (*G*) MCF-7/ADR cells, (*H*) MDA-A1 cells, (*I*) Be(2)ADR cells, and (*J*) CHO cells. Cells were incubated with 2 $\mu$M AO as described in *Materials and Methods* and examined under laser-scanning confocal microscopy. (Bar is 10 $\mu$m.)

The effect of tamoxifen on lysosomal pH was further tested with electron microscopic localization of DAMP. DAMP is a weak base that accumulates in acidic organelles. Quantification of subcellular concentration can be determined by using anti-DNP antibodies and gold-conjugated secondary antibodies (41). In the MCF-7/ADR cells, the lysosomes were heavily labeled with gold antibodies, demonstrating that they were acidic (Fig. 4*A*). The average density of gold particles was 7.02/$\mu$m$^2$ per lysosomal area. When MCF-7/ADR cells were treated with tamoxifen before incubation with DAMP, the anti-DNP labeling in the lysosomes was substantially reduced to 2.0/$\mu$m$^2$ per lysosome area (Fig. 4*B*). Similarly, with monensin treatment, the concentration fell to 0/$\mu$m$^2$ (data not shown).

The cytosolic or nuclear pH were selectively quantified by loading MCF-7/ADR cells with SNARF-conjugated to either 10-kDa or 70-kDa dextrans, respectively (42). The 70-kDa dextrans remained exclusively cytosolic. In contrast, the 10-kDa dextrans were found both within the cytosolic and nuclear compartment (38). The SNARF-conjugated dextrans are too large to cross membranes and thus are selective markers for the cytosolic and nuclear pH (rather than total cellular pH). By using this method, the mean cytosolic pH was 7.1 ± 0.1 for the MCF-7/ADR cells ($n$ = 13) and MCF-7 pH 6.65 ± 0.4 ($n$ = 16) for the MCF-7 cells (38). Thirty minutes after addition of 10 $\mu$M tamoxifen, the cytosolic pH was 0.1 units more alkaline (Table 1). Nigericin, which also reverses drug resistance (36), shifted the cytosolic pH 0.2 units more alkaline over 30 min. None of these agents had a measurable effect on nuclear pH.

**Effects of Tamoxifen on Cell Physiology.** Organelle acidification affects many cellular functions, including the sorting of lysosomal enzymes and vesicular transport. The results with a variety of fluorescent probes demonstrate that tamoxifen disrupts acidification of cytoplasmic organelles (Figs. 1–3 and Table 1). This increase of pH should produce a number of physiological consequences for the cells. The potential effects of tamoxifen were examined on vesicular transport in the endocytic and biosynthetic pathways.

*Protein transport through endocytic pathway.* Protein transport to the surface from the endocytic pathway was studied by using fluorescent-tagged holotransferrin, which enters the cell through receptor-mediated endocytosis, releases iron in endosomes, and recycles to the surface where it is released to the media as apotransferrin. Cells were loaded with BODIPY-transferrin for 20 min and transferred to dye-free medium. Cell-associated fluorescence was quantified 0, 5, 15, and 25 min later. In MCF-7/ADR cells, 50% of BODIPY-transferrin

Table 1. Effect of tamoxifen on organellar pH

| | Cytosol | Nucleus | Recycling endosomes | Lysosomes |
|---|---|---|---|---|
| MCF-7/ADR | 7.10 ± 0.1 | 7.20 ± 0.1 | 6.1 ± 0.2 | 5.2 ± 0.1 |
| + Tamoxifen | 7.20 ± 0.1 | 7.20 ± 0.1 | 6.7 ± 0.2 | 6.6 ± 0.1 |
| Change | +0.1 | 0.0 | +0.6 | >+1.4 |

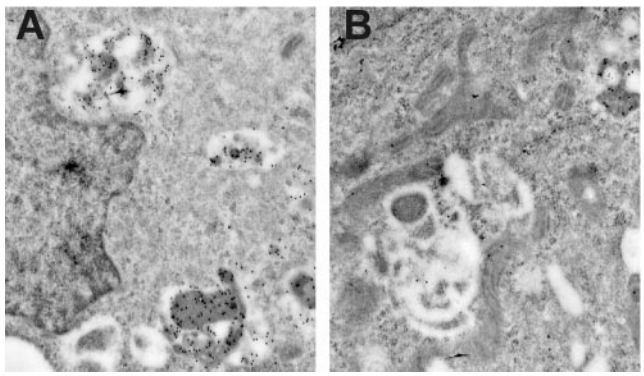


FIG. 4. Effect of tamoxifen on DAMP labeling of MCF-7/ADR cells. Acidification of the lysosomes was probed with the weak base DAMP, which accumulates in acidic organelles. (A) Electron micrograph of mouse anti-DNP and gold-conjugated anti-mouse antibodies in MCF-7/ADR cells. The gold particles indicate accumulation of DAMP within cytoplasmic organelles. The average density of gold particles was 7.02/$\mu$m$^2$ of lysosomal area. (*B*) Cells incubated with tamoxifen had a substantial reduction of anti-DAMP labeling to 2.0 gold particles/$\mu$m$^2$ of lysosomal area. Cells were incubated with DAMP, then fixed and prepared for immunoelectron microscopy as described in *Materials and Methods*. (Bar is 1 $\mu$m.)

was chased out by 5 min (Fig. 5*A*). In contrast, in the presence of 10 $\mu$M tamoxifen, it took 30 min for the concentration of intracellular BODIPY-transferrin to decrease to 50% of its steady-state level. The rate of transport of BODIPY-transferrin in MCF-7/ADR cells treated with tamoxifen was comparable with the rates of transport measured in the drug-sensitive MCF-7 cells (Fig. 5*A*). Slowed transport could be the consequence of either a direct effect on the kinetics of vesicular transport, or alternatively, it could reflect a pH-sensitive step specifically in the sorting and transport of the transferrin receptor.

*Lipid transport.* BODIPY-ceramide has been previously used to monitor the rate of lipid transport through the secretory system (44). Cells were incubated with BODIPY-ceramide, which is taken up and converted into BODIPY-sphingomyelin. The BODIPY-sphingomyelin transiently accumulates within the Golgi and is transported to the cell surface though the normal secretory pathway. The transport of BODIPY-ceramide out of the cell was followed over 2 hr. In MCF-7/ADR cells less than 25% of the sphingomyelin remained associated with a field of cells after 2 hr (Fig. 5*B*). In the presence of tamoxifen (10 $\mu$M), more than 70% of the sphingomyelin fluorescence remained associated with the cells. This rate is similar to the rate with which the sphingomyelin is transported to the surface in the drug-sensitive MCF-7 cells (Fig. 5*B*).

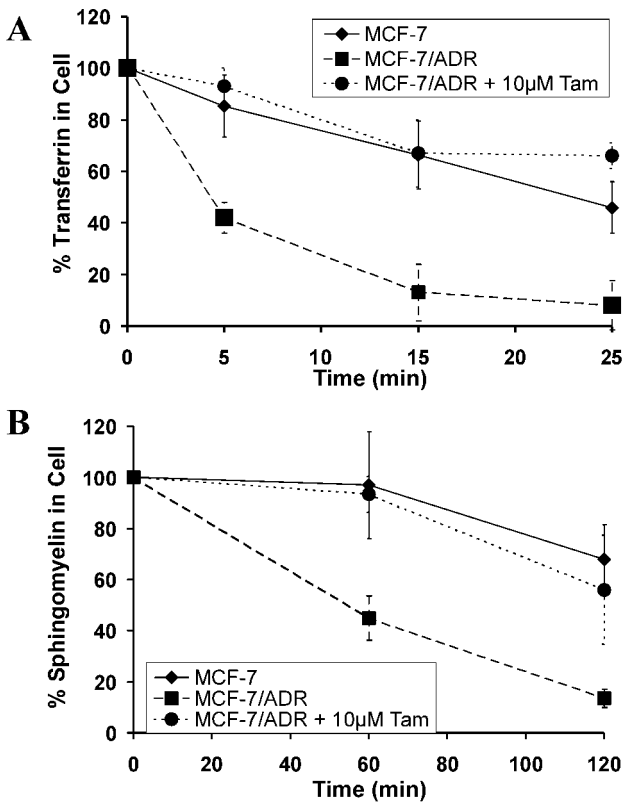


FIG. 5. Effect of tamoxifen on transport in MCF-7/ADR cells. (*A*) Kinetics of transport of BODIPY-transferrin to the surface. The cell-associated BODIPY-transferrin was quantified at various time points by using confocal microscopy. After 5 min only 50% of the transferrin was still associated with the MCF-7/ADR cells (■). In contrast, more than 90% remained with MCF-7/ADR cells that had been incubated with 10 $\mu$M tamoxifen (●). After 25 min less than 10% of the transferrin remained with the control MCF-7/ADR cells and more than 60% remained with the tamoxifen-treated cells. The rate of transferrin transport in MCF-7/ADR cells treated with tamoxifen was similar to the rate in drug-sensitive MCF-7 cells (◆). (*B*) Kinetics of transport of BODIPY-sphingomyelin to the surface. The kinetics of transport of the lipid sphingomyelin from the TGN to the surface was quantified as described in *Materials and Methods*. Two hours after removal of the BODIPY-ceramide, the fluorescence in the MCF-7/ADR cells decreased to almost 20% (■). In the presence of tamoxifen (10 $\mu$M) the BODIPY-fluorescence decrease was slower (●). In the MCF-7 cells (◆) the rate of transport of the BODIPY-sphingomyelin to the surface was similar to that of the MCF-7/ADR cells with tamoxifen.

## DISCUSSION

Tamoxifen has been demonstrated to affect many aspects of cellular and organismal physiology, including activity of secreted proteases, adhesion to extracellular matrix, responsiveness and secretion to growth factors, carcinogenic effects both *in vitro* and *in vivo*, activity of a number of membrane channels and transporters, inhibition of bone resorption, sensitivity of tumor cells to chemotherapeutics, and growth of estrogen-receptor-positive breast tumors (33). Tamoxifen usually is administered at a daily dose of 20 mg/kg body weight, and its final concentration in tissue has been reported to be 30 $\mu$M (48). Our results demonstrate that at concentrations of 0.5–10 $\mu$M, tamoxifen also can have a powerful effect directly on the acidification of cellular organelles and on transport through the secretory pathway—effects that are independent of estrogen receptors and of any potential effects of tamoxifen on transcription and protein synthesis. Many of the nonestrogen receptor-mediated effects of tamoxifen may be a direct consequence of tamoxifen blocking organelle acidification. For example, acidification by the vacuolar ATPase is essential for bone resorption (49), and acidification of cytoplasmic organelles affects accumulation of chemotherapeutics drugs (36, 38) and the sensitivity of cells to chemotherapeutics (36, 37).

Acidification is a fundamental property of normal cells and is vital to the fidelity of many cellular functions. Critical biochemical functions affected by organelle acidification include sorting of proteins between the Golgi, cell surface, endosomes and lysosomes, activation of proteins by proteases in the secretory pathway, sialylation of proteins and lipids in the Golgi, and kinetics of vesicular transport. The biochemical bases for some of these pH-sensitive effects have been identified. The mannose-6-phosphate receptor that recycles between the TGN and lysosome requires a vectorial pH gradient through the organelles to sort protein cargo from the TGN to the lysosome. In the absence of the acidification, the mannose-6-phosphate receptor is less efficient at sorting, resulting in secretion of lysosomal enzymes (50). Two enzymatic processes in the TGN function optimally at an acidic pH. Enzymatic activation of many proteins in the TGN is optimized at a pH of 5.5 (51), and the pH optimum of the $\alpha$2–6 sialytransferase is 5.5 (52). The biochemical bases for other pH-sensitive processing steps such as how acidification affects the patterns and rates of endocytosis and secretion still are unresolved (53–56).

It is tempting to speculate that the pleiotropic effects of tamoxifen are not the consequence of a multitude of mechanisms of tamoxifen action. Instead, many of these effects may be either the direct consequence of tamoxifen blocking acidification (thereby directly affecting bone resorption or sequestration of chemotherapeutic drugs away from the cytosol or activation or sorting of enzymes) or an indirect consequence of tamoxifen blocking acidification (as a result of aberrant glycosylation on cell surface receptors or secreted proteins).

A number of studies have demonstrated increased rates of tumors, especially of the endometrium and liver, in both humans and mice treated with tamoxifen. Other studies suggest that tamoxifen may enhance the effects of the carcinogen diethylnitrosamine (57). Many environmental toxins are weak bases. Tamoxifen blocks acidification of organelles (Fig. 3), resulting in the release of weak base chemotherapeutics from these organelles into the cytoplasm and nucleus (Fig. 2). Modifying this secretion-dependent mechanism of drug resis-

tance may impact on the ability of this pathway to cleanse the cell of mutagenic drugs or environmental carcinogens.

Tamoxifen is an effective agent to block the growth of estrogen-receptor-positive breast tumors. However, for the prophylactic prevention of breast cancer it may be prudent to use other inhibitors of the estrogen receptor that do not affect acidification of organelles. An understanding of the biochemical mechanism(s) for the effects of tamoxifen that are independent of the estrogen receptor could contribute to predicting side effects of tamoxifen and in designing screens to select for estrogen-receptor antagonists without these side effects.

Our gratitude goes to our colleagues Judith A. Hirsch, Denise K. Marciano, and Elliott M. Kanner for valuable comments and discussion and Helen Shio for assistance with electron microscopy. N.A. thanks the Merinoff Foundation. M.S. thanks the Pardee Foundation (Midland, MI). Y.C. was supported by National Institutes of Health Grant MSTP GM07739, and S.M.S. thanks the Keck Foundation, the Wolfensohn Foundation, the William and Helen Mazer Foundation, and the Irving A. Hansen Memorial Foundation for their support. The work was supported by American Cancer Society Grant RPG-98-177-01-CDD (S.M.S.).

1. Spiegel, D. (1997) *Semin. Oncol.* **24,** S1-36–S1-47.
2. Jaiyesimi, I. A., Buzdar, A. U., Decker, D. A. & Hortobagyi, G. N. (1995) *J. Clin. Oncol.* **13,** 513–529.
3. Early Breast Cancer Trialists' Collaborative Group (1998) *Lancet* **351**, 1451–1467.
4. Jordan, V. C. (1995) *Proc. Soc. Exp. Biol. Med.* **208,** 144–149.
5. Fisher, B., Costantino, J. P., Wickerham, D. L., Redmond, C. K., Kavanah, M., Cronin, W. M., Vogel, V., Robidoux, A., Dimitrov, N., Atkins, J., *et al*. (1998) *J. Natl. Cancer Inst.* **90,** 1371–1388.
6. Kellen, J. A. (1996) *Tamoxifen: Beyond the Antiestrogen* (Birkhäuser, Boston).
7. Marchant, D. J. (1994) *Cancer* **74,** 512–517.
8. Sasco, A. J. & Gendra, I. (1996) in *Tamoxifen: Beyond the Antiestrogen*, ed. Kellen, J. A. (Birkhäuser, Boston), pp. 59–92.
9. Lopes, M. C., Vale, M. G. & Carvalho, A. P. (1990) *Cancer Res.* **50,** 2753–2758.
10. O'Brian, C. A., Housey, G. M. & Weinstein, I. B. (1988) *Cancer Res.* **48,** 3626–3629.
11. Wiseman, H., Laughton, M. J., Arnstein, H. R., Cannon, M. & Halliwell, B. (1990) *FEBS Lett.* **263,** 192–194.
12. Ramu, A., Glaubiger, D. & Fuks, Z. (1984) *Cancer Res.* **44,** 4392–4395.
13. Trump, D. L., Smith, D. C., Ellis, P. G., Rogers, M. P., Schold, S. C., Winer, E. P., Panella, T. J., Jordan, V. C. & Fine, R. L. (1992) *J. Natl. Cancer Inst.* **84,** 1811–1816.
14. Ng, R. & Kellen, J. A. (1983) *Med. Hypotheses* **10,** 291–293.
15. Akeli, M. G., Madoulet, C., Rallet, A. & Jardillier, J. C. (1991) *Leuk. Res.* **15,** 1153–1157.
16. Maudelonde, T., Escot, C., Pujol, P., Rouanet, P., Defrenne, A., Brouillet, J. P. & Rochefort, H. (1994) *Eur. J. Cancer* **30,** 2049–2053.
17. MacNeil, S., Wagner, M. & Rennie, I. G. (1994) *Pigment Cell Res.* **7,** 222–226.
18. Mac, N. S., Wagner, M., Kirkham, P. R., Blankson, E. A., Lennard, M. S., Goodall, T. & Rennie, I. G. (1993) *Melanoma Res.* **3,** 67–74.
19. Bracke, M. E., Charlier, C., Bruyneel, E. A., Labit, C., Mareel, M. M. & Castronovo, V. (1994) *Cancer Res.* **54,** 4607–4609.
20. Croxtall, J. D., Choudhury, Q., White, J. O. & Flower, R. J. (1997) *Biochim. Biophys. Acta* **1349,** 275–284.
21. Friedl, A., Jordan, V. C. & Pollak, M. (1993) *Eur. J. Cancer* **29,** 1368–1372.
22. Huynh, H. & Pollak, M. (1994) *Biochem. Biophys. Res. Commun.* **203,** 253–259.
23. Knabbe, C., Zugmaier, G., Schmahl, M., Dietel, M., Lippman, M. E. & Dickson, R. B. (1991) *Am. J. Clin. Oncol.* **14,** Suppl. 2, S15–S20.
24. Sumida, C. & Pasqualini, J. R. (1989) *Endocrinology* **124,** 591–597.
25. Song, J., Standley, P. R., Zhang, F., Joshi, D., Gappy, S., Sowers, J. R. & Ram, J. L. (1996) *J. Pharmacol. Exp. Ther.* **277,** 1444–1453.
26. Zhang, J. J., Jacob, T. J., Valverde, M. A., Hardy, S. P., Mintenig, G. M., Sepulveda, F. V. G. D., Hyde, S. C., Trezise, A. E. & Higgins, C. F. (1994) *J. Clin. Invest.* **94,** 1690–1697.
27. Batra, S. (1990) *Cancer Chemother. Pharmacol.* **26,** 310–312.
28. Callaghan, R. & Higgins, C. F. (1995) *Br. J. Cancer* **71,** 294–299.
29. Kirk, J., Syed, S. K., Harris, A. L., Jarman, M., Roufogalis, B. D., Stratford, I. J. & Carmichael, J. (1994) *Biochem. Pharmacol.* **48,** 277–285.
30. Verrecchia, F. & Herve, J. (1997) *Pflugers Arch. Eur. J. Physiol.* **434,** 113–116.
31. Repke, K. R. & Matthes, E. (1994) *J. Enzyme Inhibition* **8,** 207–212.
32. Tonetti, D. A. & Jordan, V. C. (1996) *Mol. Med. Today* **2,** 218–223.
33. Williams, J. P., McDonald, J. M., McKenna, M. A., Jordan, S. E., Radding, W. & Blair, H. C. (1997) *J. Cell. Biochem.* **66,** 358–369.
34. Willingham, M. C., Cornwell, M. M., Cardarelli, C. O., Gottesman, M. M. & Pastan, I. (1986) *Cancer Res.* **46,** 5941–5946.
35. Moriyama, Y., Manabe, T., Yoshimori, T., Tashiro, Y. & Futai, M. (1994) *J. Biochem. (Tokyo)* **115,** 213–218.
36. Schindler, M., Grabski, S., Hoff, E. & Simon, S. M. (1996) *Biochemistry* **35,** 2811–2817.
37. Hurwitz, S. J., Terashima, M., Mizunuma, N. & Slapak, C. A. (1997) *Blood* **89,** 3745–3754.
38. Altan, N., Chen, Y., Schindler, M. & Simon, S. M. (1998) *J. Exp. Med.* **187,** 1583–1598.
39. Ghosh, R. N. & Maxfield, F. R. (1995) *J. Cell Biol.* **128,** 549–561.
40. Yamashiro, D. J. & Maxfield, F. R. (1987) *J. Cell Biol.* **105,** 2723–2733.
41. Barasch, J., Kiss, B., Prince, A., Saiman, L., Gruenert, D. & Al-Awqati, Q. (1991) *Nature (London)* **352,** 70–73.
42. McNeil, P. L., Murphy, R. F., Lanni, F. & Taylor, D. L. (1984) *J. Cell. Biol.* **98,** 1556–1564.
43. Dunn, K. W., McGraw, T. E. & Maxfield, F. R. (1989) *J. Cell. Biol.* **109,** 3303–3314.
44. Pagano, R. E., Martin, O. C., Kang, H. C. & Haugland, R. P. (1991) *J. Cell. Biol.* **113,** 1267–1279.
45. Ciocca, D. R., Adams, D. J., Bjercke, R. J., Edwards, D. P. & McGuire, W. L. (1982) *Cancer Res.* **42,** 4256–4258.
46. Berglindh, T., Dibona, D. R., Ito, S. & Sachs, G. (1980) *Am. J. Physiol.* **238,** G165–G176.
47. Debenham, P. G., Kartner, N., Siminovitch, L., Riordan, J. R. & Ling, V. (1982) *Mol. Cell Biol.* **2,** 881–889.
48. Dragan, Y. P., Fahey, S., Nuwaysir, E., Sattler, C., Babcock, K., Vaughan, J., McCague, R., Jordan, V. C. & Pitot, H. C. (1996) *Carcinogenesis* **17,** 585–594.
49. Nordstrom, T., Shrode, L. D., Rotstein, O. D., Romanek, R., Goto, T., Heersche, J. N., Manolson, M. F., Brisseau, G. F. & Grinstein, S. (1997) *J. Biol. Chem.* **272,** 6354–6360.
50. Pohlmann, R., Kruger, S., Hasilik, A. & von Figura, K. (1984) *Biochem. J.* **217,** 649–658.
51. Rhodes, C. J., Brennan, S. O. & Hutton, J. C. (1989) *J. Biol. Chem.* **264,** 14240–14245.
52. Keller, S. J., Keenan, T. W. & Eigel, W. N. (1979) *Biochim. Biophys. Acta* **566,** 266–273.
53. Tartakoff, A. M. (1983) *Cell* **32,** 1026–1028.
54. Parczyk, K. & Kondor-Koch, C. (1989) *Eur. J. Cell Biol.* **48,** 353–359.
55. Mellman, I., Fuchs, R. & Helenius, A. (1986) *Annu. Rev. Biochem.* **55,** 663–700.
56. Sakaguchi, T., Leser, G. P. & Lamb, R. A. (1996) *J. Cell Biol.* **133,** 733–747.
57. Dragan, V. P., Vaughan, J., Jordan, V. C. & Pitot, H. C. (1995) *Carcinogenesis* **16,** 2733–2741.